https://doi.org/10.5194/essd-2026-56
Preprint. Discussion started: 31 March 2026
© Author(s) 2026. CC BY 4.0 License.

Open Access Earth System Science Data Discussions

Regional flood hazard mapping for February 2023 Ex-Tropical Cyclone Gabrielle, New Zealand.

Joë Pelmard[1], Emily M. Lane[2], Alice Harang[2], Cyprien Bosserelle[2], Zhonghou Xu[3], Rose Pearson[2], Trevor Carey-Smith[4], Graeme Smart[2], Jochen Bind[2], Raghunathan S. Kumar[2], Elvira Cheng[2], Giang Bui[2], Ryan Paulik[3], Conrad Zorn[1], Liam Wotherspoon[1]

[1]Department of Civil and Environmental Engineering, University of Auckland, Auckland 1142, New Zealand
[2]Earth Sciences New Zealand, Christchurch 8011, New Zealand
[3]Earth Sciences New Zealand, Hamilton 3216, New Zealand
[4]Earth Sciences New Zealand, Wellington 6021, New Zealand

Correspondence to: Joë Pelmard (joe.pelmard@auckland.ac.nz), Emily M. Lane (emily.lane@niwa.co.nz)

Abstract. On February 13th to 14th 2023 ex-Tropical Cyclone Gabrielle (ETC Gabrielle) caused widespread flooding in Aotearoa New Zealand. The dataset presented is a collection of simulations representing the hydrodynamics response of 16 locations across the Hawke's Bay and Tairāwhiti regional districts to ETC Gabrielle. Using gridded hourly rainfall derived from rainfall gauges, an end-to-end hydrodynamic modelling framework was applied to generate 16 inundation models with variable grid resolutions from 64 m to 4 m. The framework includes: (i) the identification of contributing river networks and catchments from an initial outline of the regions of interest, (ii) reconstruction of the DEM and surface roughness map, (iii) extraction of the rainfall, (iv) hydrological modelling in the upper catchments to estimate input river hydrographs, and (v) hydrodynamic modelling on the lower catchment. These models were calibrated and validated against hydrograph records (temporal accuracy), as well as post-event aerial imagery and in-situ high-water mark surveys (spatial accuracy) where available. With the increasing frequency of extreme weather events, this spatio-temporally detailed and methodologically consistent dataset offers valuable insights for researchers and stakeholders on the implications of large-scale flood events and will support efforts to enhance protective and preventive measures as well as post hoc analysis of direct and indirect impacts (e.g., building and infrastructure physical damage), while the model framework can be employed to simulate flood maps for future events. The dataset is available at https://doi.org/10.5281/zenodo.17986628 (Pelmard, 2025a) for the Tairāwhiti regional district and https://doi.org/10.5281/zenodo.18001575 (Pelmard, 2025b) for the Hawke's Bay regional district.

1 Background and summary

From February 12 to 16 2023 Ex-tropical Cyclone Gabrielle (henceforth referred to as Cyclone Gabrielle) struck Aotearoa New Zealand at a national scale, quickly standing out as one of the worst flood disasters recorded in the country. Peak impacts occurred on February 13 and 14 in the eastern North Island and Northland, when rainfall reached up to 500 mm over 12 hours, far exceeding the local authorities' expectations, and rapidly overwhelming local emergency response capabilities (Fig. 1).

https://doi.org/10.5194/essd-2026-56
Preprint. Discussion started: 31 March 2026
© Author(s) 2026. CC BY 4.0 License.

The event caused 11 fatalities, with nearly 2,000 people injured and hundreds of others exposed to life-threatening situations due to the rapid water level rise. Additionally, over 200,000 households lost power at the peak of the event and there was extensive damage to buildings, including more than 400 buildings later deemed uninhabitable and over 3,000 having suffered moderate damage across the North Island (Wilson et al., 2023). As of June 1st 2023, the total insurance claim cost estimates exceeded NZD $1.8 billion across all sectors for 58,848 claims – more than 5 times the annual extreme weather events costs in the previous years (Te Kāhui Inihua o Aotearoa Insurance – Council of New Zealand 2023, 2024). Overall, the combined recovery costs due to cyclone Gabrielle and the Auckland Anniversary weekend floods that struck two weeks prior were estimated to range anywhere between NZD $9 to $14.5 billion, with disruptions lasting several months and full recovery expected to take years (Wilson et al., 2023).

The Hawke's Bay and Tairāwhiti regions were among the most severely hit (Hawke's Bay Regional Council, 2024; Trust Tairāwhiti, 2023) (area bounded by the catchment outlines in Fig. 1). Together, they accounted for close to 70% of the national insurance claims all sectors included on September 1st 2023 (Te Kāhui Inihua o Aotearoa Insurance – Council of New Zealand 2023), with over 70% of the country's damaged buildings and the total damage claims to private housing exceeding NZD $450 million. The economy in these regions, predominantly organized along riverbanks and deeply rooted in agriculture, was severely impacted. The large inland runoffs and silt that was deposited inflicted substantial losses to the agricultural, horticultural and viticultural production, and the effects of land and equipment damage (machinery, fencing…) are expected to last for years.

Entire communities were flooded – a stark example being the Esk Valley, where spectacular flash floods submerged the area in over 5m of turbid water, with more than 2m of silt deposits remaining after the water receded (Hawke's Bay Regional Council et al., 2023). In Wairoa, where the community was still recovering from flooding from the previous year, a third of the 1,500 houses were damaged (Wilson et al., 2023). Failure of critical infrastructure emphasized the vulnerability of the regions to flood hazards and revealed the multi-scale impacts of such events. Levees breaches at more than 30 locations along the two major rivers of the Heretaunga Plains intensified flooding in already severely impacted areas. Multiple roads and bridges were washed away and, in Tairāwhiti, 90% of the communication towers were out of service during the peak of the event, further isolating the population and blocking emergency response routes.

This overview reveals the urgent need to assess and understand flood hazards at both local and regional scales, not only to better characterize the affected areas and guide post-event response activities, but also qualify the indirect impacts. As a first step towards the development of a methodologically consistent nationwide mapping of flood hazards, we present here a dataset of simulations capturing flooding in the most affected areas in the Hawke's Bay (Pelmard, 2025b) and Tairāwhiti (Pelmard, 2025a) regional districts during Cyclone Gabrielle. The models were developed as part of the "Rapid Flood Hazard Modelling for Cyclone Gabrielle Recovery" plan, a collective initiative involving district councils, research institutes, and private contractors aiming to lead a comprehensive mapping of the flood hazards during the event. The plan aimed to leverage existing modelling resources developed by Earth Sciences New Zealand (ESNZ) – ex–National Institute of Water and Atmospheric Research (NIWA) – to develop a set of methodologically consistent hydrodynamic models.

https://doi.org/10.5194/essd-2026-56
Preprint. Discussion started: 31 March 2026
© Author(s) 2026. CC BY 4.0 License.

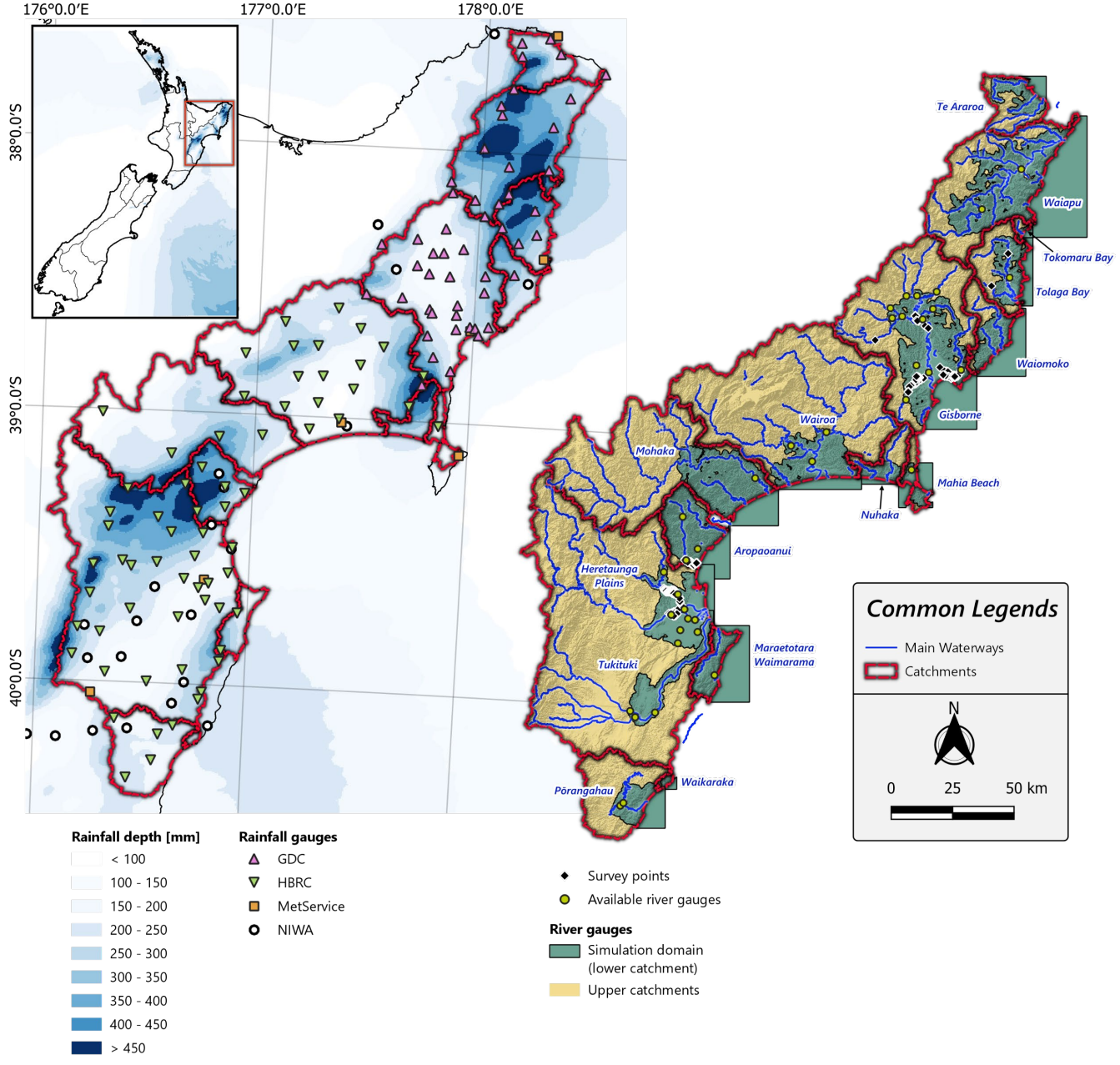

Figure 1: Numerical models presentation: 24-hour VCSN climate network cumulated rainfall for the period ending 2023-02-14 09:00:00 (*a*), across the simulated catchment in the Hawke's Bay (HBRC) and Tairāwhiti regional districts (GDC) (*b*) and simulation domains and corresponding catchment areas (*c*).

https://doi.org/10.5194/essd-2026-56
Preprint. Discussion started: 31 March 2026
© Author(s) 2026. CC BY 4.0 License.

2 Study area

The Hawke's Bay and Tairāwhiti regional districts are located on the eastern side of the North Island. Topography, population density and land use are shown in Fig. 2a-b. The landscape is characterised by long mountain ranges which rise toward the western edge of the regions, reaching 500 m to 1200 m at their highest points (Fig. 2a). The elevation decreases rapidly towards the coast, with narrow floodplains and short hydrological river response times – flooding in the lower river reaches typically occurs within hours following peak rainfall.

While higher elevations are covered by indigenous forests, the land is predominantly composed of grassland used for pasture, followed by areas of shrubland, scrub, and exotic forest primarily managed for timber production (Fig. 2b), particularly prone to rainfall-induced landslides and surface runoff erosion. The resulting sediment and coarse debris (e.g. woody debris) transport in river flows contributes to substantial channel aggradation after peak rainfall and exacerbates flood impacts in cultivated and populated areas. A comprehensive database of human-mapped landslides triggered by Cyclone Gabrielle compiles over 160,000 landslides across the affected regions, with highest densities in Hawke's Bay and Tairāwhiti (Leith et al., 2025; Massey et al., 2025).

The population is scarce and, together, the regions account for less than 5% of the total population of the country. Outside the main urban centres of Gisborne (38 300 inhabitants) and the Napier-Hastings urban conglomeration (156 000 inhabitants), which account for over 70% and 85% of their respective district populations (Stats NZ – Tatauranga Aotearoa (n.d.), 2023), the settlements range from small communities of a few dozen residents to larger townships of several thousand inhabitants. The dispersion of the population poses significant challenges for emergency response coordination and efficient resource allocations during extreme events, and Cyclone Gabrielle starkly highlighted the vulnerability of these regions to flood hazards. Settlements are concentrated along major rivers flowing through valleys carved between the mountains with limited transport network redundancy, and the indigenous Māori population, approximately half of the total regional population, often resides in areas critically exposed to natural hazards. Many local communities, particularly those geographically isolated, frequently experience damage and disruption from recurring flood events.

Despite the relative low population, the regions are instrumental to the national food supply, Hawke's Bay being known as the "fruit bowl" of Aotearoa New Zealand. These areas have historically been favoured for their fertile soils enriched over time with alluvial deposits by repeated overflow of the main rivers. Today, crop and pasture lands compose most of the valley floors and riversides. However, the very nature of these developed arable lands makes them particularly vulnerable to flood risk.

https://doi.org/10.5194/essd-2026-56
Preprint. Discussion started: 31 March 2026
© Author(s) 2026. CC BY 4.0 License.

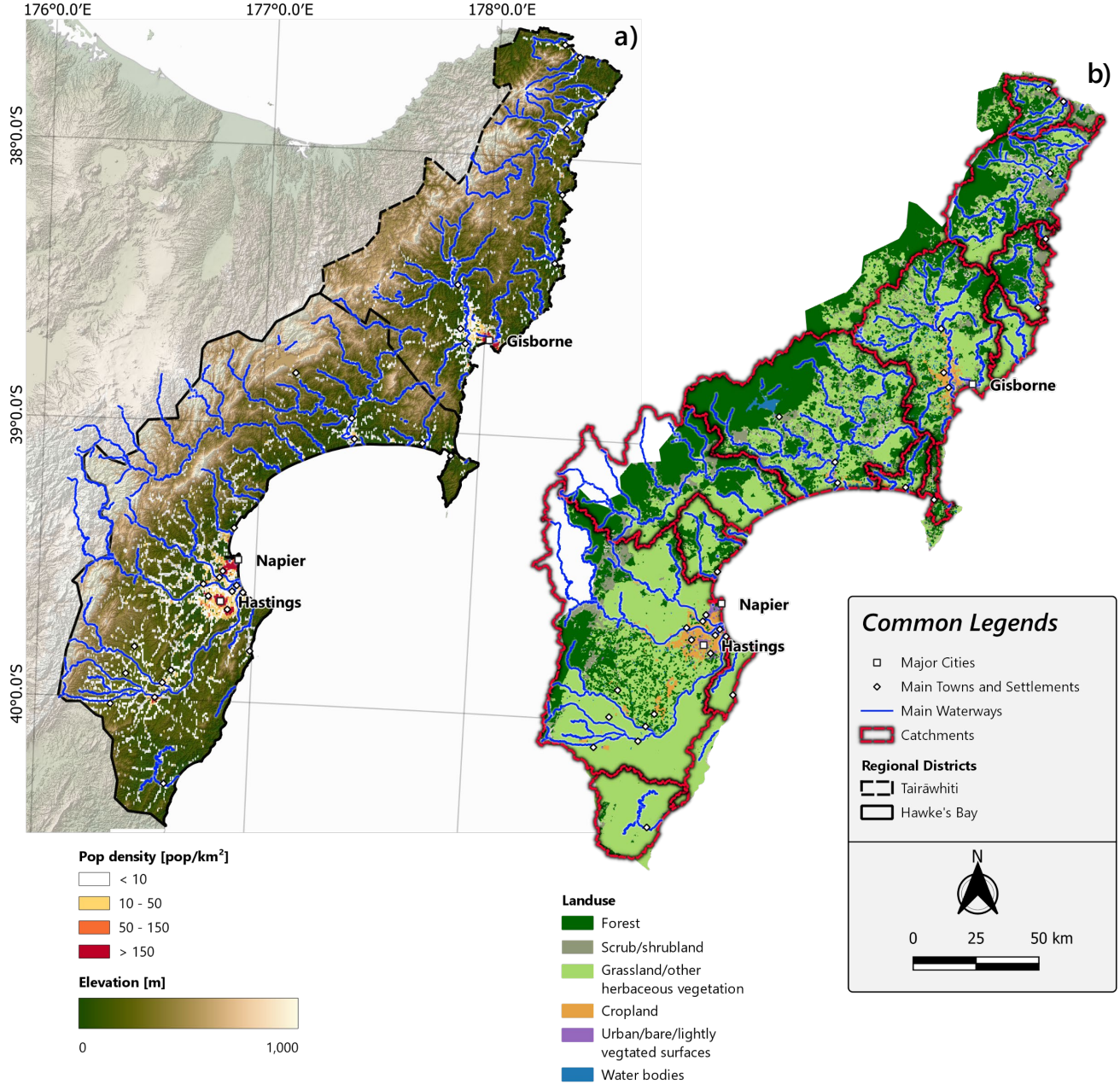

Figure 2: Regional population density (Stats NZ – Tatauranga Aotearoa (n.d.), 2023) (*a*) and broad land cover classes (*b*) across the Hawke's Bay and Tair āwhiti regional districts.

100

https://doi.org/10.5194/essd-2026-56
Preprint. Discussion started: 31 March 2026
© Author(s) 2026. CC BY 4.0 License.

Open Access Earth System Science Data Discussions

Table 1. List of domains and simulation cases, including calibrated models and scenarios. Domains are presented from North to South following the coastline.

Domains	Main Waterways	Domain/Catchment areas	River gauges	
Te Araroa	Karakatuwhero River Wharekahika River Awatere River	136 km^2 / 434 km^2	0	
Waiapu	Waiapu River and tributaries (Poroporo, Mangaoparo, Tapuaeroa and Mata Rivers)	818 km^2 / 1873 km^2	2	1 located in the upper catchment
Tokomaru Bay	Mangahauini River	6 km^2 / 43 km^2	0	
Tolaga Bay	Ūawa River	190 km^2 / 604 km^2	1	Located in the upper section of the domain
Waiomoko	Pakarae River Waiomoko River	198 km^2 / 417 km^2	0	
Gisborne	Waimatā River Waipaoa River	795 km^2 / 2648 km^2	12	1 failed before the peak
Mahia Beach	Whangawehi Stream	71 km^2 / 159 km^2	1	Located in the upper section of the domain
Nuhaka	Nūhaka River Tahaenui River	83 km^2 / 278 km^2	0	
Wairoa	Wairoa River	411 km^2 / 3947 km^2	3	
Mohaka	Mohaka River	556 km^2 / 2831 km^2	1	
Aropaoanui	Esk River Aropaoanui River Te Ngarue Stream	473 km^2 / 557 km^2	3	2 failed before the peak
Heretaunga Plains	Ngaruroro River Tūtaekurī River Tukituki River	540 km^2 / 6024 km^2	9	**Major rivers.** 1 failed after the peak in the upper region and 2 failed during the rising limb **Minor rivers.** 2 failed during the rising limb and 1 washed away by levee breaching runoff
Tukituki	Tukituki River Waipawa River	253 km^2 / 2507 km^2	3	All 3 in the Upper section of the domain
Maraetotara-Waimarama	Maraetotara River, Pouhōkio River	247 km^2 / 256 km^2	1	
Waikaraka		12 km^2 / 27 km^2	0	
Pōrangahau	Pōrangahau River Mangaorapa Stream	175 km^2 / 860 km^2	3	2 failed during the rising limb

3 Methods

3.1 Simulation domains

Sixteen domains were selected to represent floodplains of the major water catchments based on population and economical exposure. The domains are introduced in Table 1 and their locations are identified by the lower catchments in Fig. 1b. The inland cover of the simulation domains varies from 6 km^2 to 820 km^2, with an average area of 275 km^2, for associated catchment areas varying from 27 km^2 to 6025 km^2, with an average of 1650 km^2.

https://doi.org/10.5194/essd-2026-56
Preprint. Discussion started: 31 March 2026
© Author(s) 2026. CC BY 4.0 License.

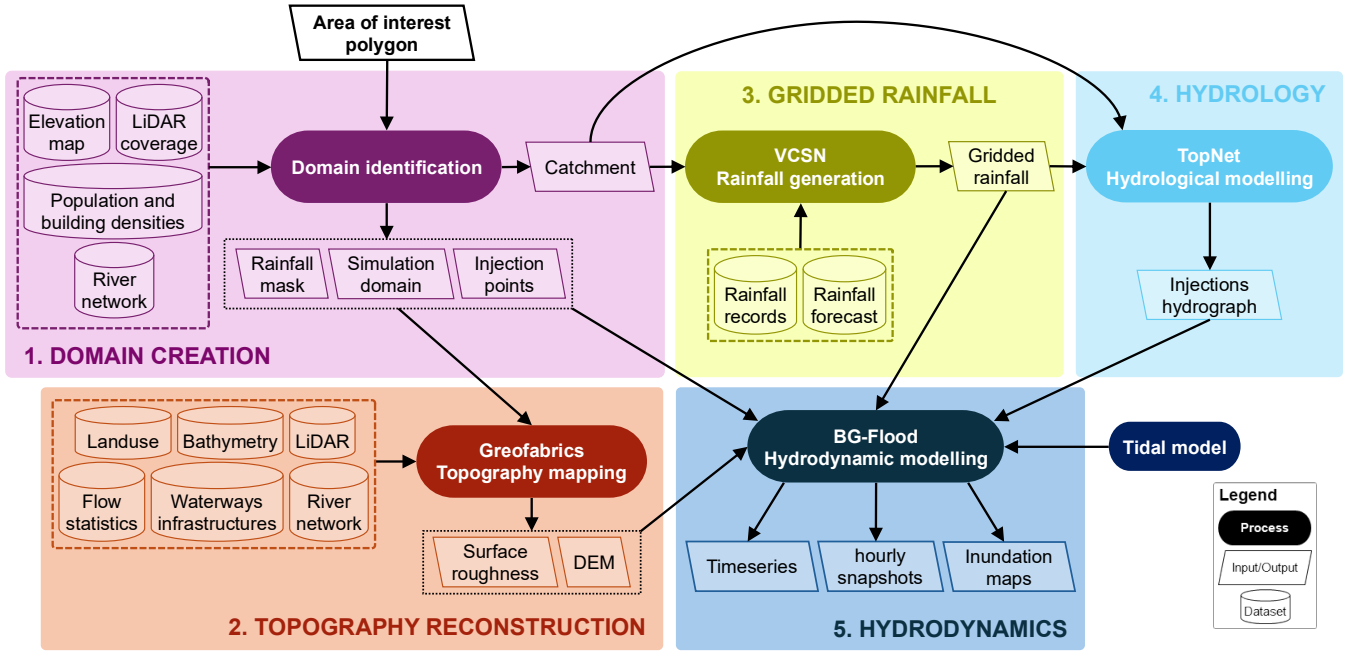

Figure 3: Flood modelling framework flowchart.

3.2 Numerical framework

The input data and hydrodynamic models are generated using the in-house framework developed by NIWA, using pre-event topographical data. The framework is operated using the Cylc engine workflow scheduler (Oliver et al., 2019; Oliver et al., 2018) and combines five steps (Fig. 3): (i) the derivation of the simulation domain, catchment and rain-on-grid masks from an initial specified polygon roughly delineating the area of interest, (ii) the generation of hydraulically conditioned DEM and surface roughness maps, (iii) the estimation of gridded rainfall from rainfall gauge records (iv) hydrological modelling on the catchment to estimate hydrographs at river flow injections, (v) hydrodynamic modelling on the floodplain.

3.3 Domain creation

The domain is created by refining an area of interest polygon that roughly delineates the locations of interest through the compilation of geographical data – shoreline, LiDAR coverage, population and building density – and river catchment data extracted from the River Environment Classification v2.5 database (REC2.5) (Earth Sciences New Zealand, 2022). REC2.5 is a digital river network which compiles the river reaches, their associated sub-catchments and other collated geographic and topographic information. Four polygon masks are created (Fig. 4): the water catchment, the lower catchment, the rainfall mask and the hydrodynamics simulation domain.

1. The water catchment area feeding into the location of interest is identified by following the REC2.5 network for each river within the area of interest polygon up to its headwaters to include all the sub-catchments flowing into it.

https://doi.org/10.5194/essd-2026-56
Preprint. Discussion started: 31 March 2026
© Author(s) 2026. CC BY 4.0 License.

2. The water catchment is split into two regions, the lower catchment corresponding to the floodplain of interest, and the upper catchment where the river flows are evaluated using the surface runoff hydrological model. The lower catchment is a refined version of the initial area of interest polygon and is generated by aggregating sub-catchments as identified in REC2.5 within the area of interest polygon with bed slope < 20°, population densities > 0.00004 inhabitant/km^2 and building densities > 0.00008 building/km^2. The borders of the lower catchment connect river injection points identified as the locations where the rivers enter the domain and are labelled by their corresponding river reach ID in REC2.5.
3. The rainfall mask defines the region where the rainfall forcing is applied in the hydrodynamic model. It is created by extending the lower catchment along the coastline and offshore, using the lower catchment's coordinates extrema as bounding limits.
4. The hydrodynamics simulation domain is created as a 500 m buffer around the rainfall mask. The buffered cells act as ghost cells used to ensure numerical stability at the river injection boundaries (see Sect. 3.7.2).

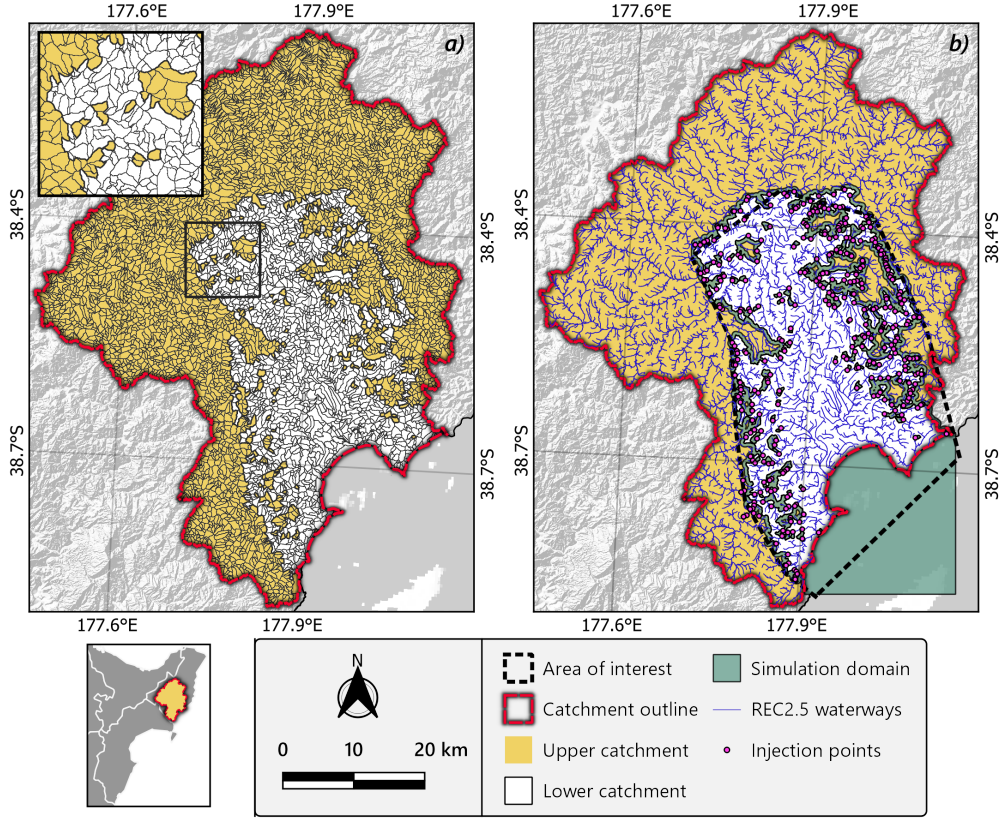

Figure 4: Domain generation presentation for the Gisborne domain. Lower and upper catchments overlaid with the REC2.5 sub-catchment network with inset at the transition lower/upper catchment (*a*), and initial area of interest, catchment, lower catchment, simulation domain and injection points (*b*).

https://doi.org/10.5194/essd-2026-56
Preprint. Discussion started: 31 March 2026
© Author(s) 2026. CC BY 4.0 License.

3.4 Topography reconstruction

The modelling is performed using pre-event topographical data. Hydraulically conditioned DEMs and roughness maps are generated for the entire country as a tileset of 425 tiles of 30 km×30 km at 8 m×8 m resolution using the open-source GeoFabrics procedure (Pearson et al., 2023). The topographical data are reconstructed from the collation of the most recent LiDAR survey points available on the open access online platform OpenTopography (Hawke's Bay Regional Council et al., 2023; Gisborne District Council and Toitū Te Whenua – Land Information New Zealand (LINZ), 2021) leading up to the event, the REC2.5 river network, and a dataset of offshore, estuarine and river elevations curated by Earth Sciences New Zealand (ESNZ) where available.

In addition, the DEMs are hydraulically conditioned to open waterways and remove obstructions captured by the remote sensing elevation data (e.g. bridges, culverts, thick vegetation covering waterways). A range of techniques are used to reconstruct the river bathymetry for major rivers that lack gridded bathymetry data. For rivers with localized cross-section elevation surveyed data, Geofabrics interpolates the riverbed elevation between the surveyed sections using the riverbanks as the sections' endpoints. In the absence of bathymetric information, the riverbed is estimated using the uniform flow approach introduced by Neal et al. (2021). In this case, the river width and slope are directly evaluated from the LiDAR records, and the cross-section shape is derived from the mean-annual flood flow and Manning's roughness coefficients prescribed along the rivers' centreline as a shapefile. Finally, river mouths are opened to reproduce the rivers opening section during peak discharge using the uniform flow approach.

The elevation maps resolution is chosen to find the best compromise between resource allocation and accurate representation of the landscape. Overall, 8 m resolution DEMs are found to be sufficiently fine to capture most determinant topographical features constraining the flow, except at locations where sharp elevation gradients tend to flatten topographical features with transverse dimensions of the same order of magnitude as the elevation map resolution, in the present case flood protection levees. With a typical levee width varying between 5 m and 15 m in New Zealand, their cross-sections extend over 1 to 3 cells in the 8 m DEM. Comparison to the input 1 m LiDAR shows levees crest elevation differences reaching up to 0.4 m, which critically impacts the results when the river reaches approach critical flood threshold. According to the the New Zealand Inventory of Stopbanks (NZ idiom for levees) (NZIS) polylines database (Crawford-Flett et al., 2022), the Heretaunga Plains (166 km of levees) and Gisborne domains (87 km of levees) account together for over 90% of the total levees in length. In comparison, Mahia beach, the third domain with the longest levee network count roughly 5km of levees mostly constrained to the upper reaches of the simulation domain. Consequently, additional topographical conditioning were also applied in these two domains.

https://doi.org/10.5194/essd-2026-56
Preprint. Discussion started: 31 March 2026
© Author(s) 2026. CC BY 4.0 License.

3.4.1 Topography conditioning in the Heretaunga Plains and Gisborne

In Gisborne where levees are localised along the lower half of the Waipaoa River, the 8 m resolution DEM was conditioned to correct the levees crest elevation with the corresponding LiDAR values. For each cell representing a levees crest, the LiDAR points elevation were extracted and the new cell value was chosen as their maximum.

For the Heretaunga Plains where the levee network is more complex, a 4 m DEM was generated and used instead of the 8 m DEM. In addition, the roughness map was also locally corrected to account for flow obstructions due to the large accumulation of at the Brookfield bridge piers (Tūtaekurī River). After calibration, an appropriate surface roughnes of 4 m across the river channel was chosen, which corresponds to a physical obstruction of approximately half the channel depth.

3.5 Gridded rainfall

The hourly rainfall data for the period 2023-02-11 22:00:00 to 2023-02-16-21:00:00 is estimated across the Hawke's Bay and Tairāwhiti regions on a Virtual Climate Station Network (Tait et al., 2006) with a resolution of approximately 500 m×500 m. Collated rainfall observations from gauges operated by NIWA, the national meteorological agency MetService, and the Hawke's Bay regional council and Gisborne district council (Fig. 1) are interpolated onto the grid using a thin-plate smoothing spline interpolation, with rainfall forecast of the event generated using the New Zealand Convective Scale Model (Revell et al., 2019) on a 1.5 km×1.5 km resolution grid as spatial co-variate. In this way, realistic rainfall patterns calibrated by rain gauge observations capture patterns of where the highest rainfall is expected. Observations from citizen rain gauges collated by Hawkes Bay Regional Council are included in a second iteration of the interpolation.

3.6 Hydrology

The hydrographs (m^3/s) at the injection points as represented in Fig. 4 are generated using the comprehensive hydrological rainfall-runoff model TopNet used and calibrated in Aotearoa New Zealand for over 20 years (McMillan et al., 2016). TopNet simulates over a digital river network based on sub-catchments with associated hydrological and topographical data (in this case REC2.5 was used).

Using the gridded hourly rainfall alongside with quantities describing ambient atmospheric conditions (e.g. temperature and relative moisture), the model simulates the regions' hydrology over the REC2.5 digital river network (Earth Sciences New Zealand, 2022) to generate hydrographs for each river reach referenced in REC2.5. Additional hydrological and topographical data are directly extracted from characteristic values associated to each sub-catchment in the REC2.5 database. To ensure realistic antecedent conditions including river flows and soil moisture, the regional model is first spun up over a period of 5 years forced by hourly gridded historical VCSN data. This spin-up is especially important given the generally wet soil conditions preceding the event, caused by persistent rainfall following Cyclone Hale that occurred a month earlier (2023-01-07 to 2023-01-12). This model is then forced by the specially created Cyclone Gabrielle event VCSN to generate hydrographs over the entire region.

https://doi.org/10.5194/essd-2026-56
Preprint. Discussion started: 31 March 2026
© Author(s) 2026. CC BY 4.0 License.

Open Access Earth System Science Data Discussions

205 ## 3.7 Hydrodynamics

3.7.1 Hydrodynamics solver

The simulations are performed using the 2D open-source GPU-enabled numerical solver BG-Flood (Block-adaptative on Graphics processing unit Flood model) (Bosserelle et al., 2020; Xu et al., 2025). BG-Flood solves the 2D shallow water equations using a version of the Saint-Venant solver implemented in the open-source modelling framework Basilisk (Popinet,
210 2011). It uses a Block-Uniform Quadtree structure (Vacondio et al., 2017) designed to leverage the inherent parallel computing capabilities of graphic processing units (GPU) while offering cost-effective allocations of the computational resources by allowing targeted grid refinement in locations of interest. Unlike The grid refinement is set at the beginning of the simulation and remains static throughout. The surface friction is modelled using Manning's formulation with an equivalent Manning's roughness coefficient calculated using the dynamic roughness length model by Smart (2018). This formulation has been
215 successfully applied to a broad range of New Zealand river conditions and reported overall better velocity predictions than Manning's equation using constant Manning's coefficient (Smart (2018, 2004).

3.7.2 Boundary conditions

Inland domain boundaries are treated as impermeable walls to avoid water exiting the domain upstream of the injection points. The ghost cells within the 500 m buffered region around the lower catchment are added to the numerical model to prevent the
220 growth of numerical instabilities due to water accumulations at the inland solid wall boundaries. Open-sea tidal boundary conditions are implemented as absorption boundaries, which impose time-varying water surface elevation while allowing outward propagating surface waves to exit the domain freely. The timeseries of tidal sea surface elevation are interpolated from sea level forecasts (Lane et al., 2009; Lane and Walters, 2009) at points located offshore of major river mouths on the Hawke's Bay and Tairāwhiti coastlines.

225 ### 3.7.3 Grid resolution

BG-Flood uses a Block-Uniform Quadtree structure (Vacondio et al., 2017). This approach enables local refinement of the mesh, while retaining the block structure traditionally used with GPUs to facilitate memory indexing and parallel computing allocations regardless of the refinement. Firstly, an initial uniform grid (level 0) of cell size dx_0 is constructed and divided into blocks of 8×8 cells. Unlike traditional uniform quad-tree grid sets where the cells are directly divided to increase the resolution,
230 refinement is here achieved by iteratively dividing the blocks into 4 blocks of 8×8 cells until achieving the desired level of refinement. The cell size after n consecutive cell divisions reduces to $dx/2^n$.

Refinement is prescribed as a refinement map indexing the level of refinement across the simulation domain. The baseline procedure for the definition of the refinement map is twofold. Firstly, a preliminary coarse simulation on a regular square grid with a resolution of 32 m resolution is conducted to identify the outline of the flooded areas. These coarse results are used to
235 define a refinement map ranging from level 0 to 4 as follow

https://doi.org/10.5194/essd-2026-56
Preprint. Discussion started: 31 March 2026
© Author(s) 2026. CC BY 4.0 License.

Open Access Earth System Science Data Discussions

$$dx_n = {dx_0}/{2^n} \; with \quad n = \begin{cases} 4 \; in \; a \; 10 \; m \; buffer \; zone \; around \; levees \\ 3 \; if \; h_{max} > 0.1 \; m \; and \; vmax > \; 0.5 \; {m}/{s} \\ 2 \; if \; h_{max} > 0.1 \; m \; and \; vmax < \; 0.5 \; {m}/{s} \\ 0 \; elsewhere \end{cases}, \tag{3.1}$$

with $dx_0 = 64\ m$. Level 4 is imposed to ensure accurate capture of the levees crest elevation, and the levees' locations are extracted from the New Zealand Inventory of Stopbanks (NZIS) polylines shapefile (Crawford-Flett et al., 2022).

4 Modelling strategy

Modelling is done in two phases: In the first phase, baseline hydrodynamic models are developed following the workflow procedure outlined in Sect. 3. In the second phase, calibration and scenario are performed to refine the hydrodynamic models predictions and explore additional scenarios.

4.1 Baseline modelling and validation

Separate models are created for each domain. Simulations are validated using the best observational data for each domain. Flood extents are qualitatively assessed by comparing the predicted inundation maps with post-event aerial and satellite imagery available on the Land Information New Zealand Data Service (LINZ) platform (Toitū Te Whenua – Land Information New Zealand Data Service (LINZ), 2023c, a, b). For each domain, the highest-quality image set is selected based on resolution and visibility (e.g. cloud cover, shading). Where available, predicted water level timeseries are compared with hydrograph records from river gauges operated by NIWA and the local councils to assess temporal accuracy. In addition, high-water marks were surveyed at six locations across three domains – the Heretaunga Plains, Aropaoanui and Gisborne (see Fig. 1b) – and are compared to the corresponding predicted maximum water depths.

4.1.1 High-water marks validation

The prediction accuracy at surveyed high-water marks is assessed through the direct analysis of the modelling error rather than correlation-based statistics relating modelled and surveyed water surface elevations. Traditional correlation measures, such as linear regression and coefficient of determination (r^2), are sensitive to elevation variations when the surveyed terrain spans large elevation ranges relative to the prediction error, rendering direct correlation metrics ineffective to qualify the model accuracy at domains' scale. In the present cases, ground elevation differences across the surveyed points exceed the prediction error by more than one order of magnitude in each domain, resulting in artificially high correlations, regardless of the amplitude of the prediction errors.

Introducing $\eta_{max} = z_b + h_{max}$ and η_{HWM} as the predicted maximum water surface and high-water mark elevations, respectively, the prediction error ε is defined as

https://doi.org/10.5194/essd-2026-56
Preprint. Discussion started: 31 March 2026
© Author(s) 2026. CC BY 4.0 License.

$$\varepsilon = \eta_{s,max} - \eta_{HWM} \quad (4.1)$$

For each surveyed point, η_{max} are extracted from the gridded map at the point coordinates when wet, or from the nearest wet grid cell when dry.

To characterise the statistical distribution of ε, we propose the use of scaled kernel density estimations (KDE), a non-parametric method for estimating the probability density function of a random variable. Gaussian kernels are first applied to each sample point, then summed to form a continuous density estimate. Unlike histograms, whose visual representation depend on the bin widths and the bins edge values, KDE is a continuous estimate and the curve smoothing is controlled by the Gaussian kernel bandwidth parameter, providing a more flexible and less discretization-dependent estimate of the underlying distribution. The normalised KDE is rescaled to integrate to the total number of observations, providing a continuous measure of the error intensity.

Two metrics are here used to assess the predictions: the median error characterising the general model bias; the 80% central error range [P_{10}; P_{90}] expressing the dispersion of ε about its median.

4.2 Calibration

Following the initial validation, a second modelling phase is undertaken to address discrepancies in the baseline results. Considering the regional scale of the models, calibration is minimal and focused on two main objectives

- Correcting uncertainties in gridded rainfall inputs caused by sparse observational data coverage and interpolation assumptions, particularly in mountainous upper catchments where low gauge density leads to misevaluations of rainfall peaks intensities and locations (discussed in Sect. 6.2). This is achieved
    a. at the lower catchment level by scaling targeted or all river injections entering the domains
    b. at the catchment level by scaling the gridded rainfall over the whole catchment.
- Dynamically modifying the topography to implement levee breaches during the simulation period in the Heretaunga Plains.

Calibration is constrained by the quality and availability of validation data: six domains contain no river gauge stations, only two count more than five stations in their lowest sections, and surveyed high-water marks are available in three domains already well covered with gauges. Consequently, detailed calibration is carried out only for domains with sufficient data to ensure reliable corrections. In some cases, additional models are derived from the best-performing models (baseline or calibrated) to investigate location specific processes (e.g. impact of inundation protection wall along the Tukituki River). Additional simulated cases are summarized in Table 3.

https://doi.org/10.5194/essd-2026-56
Preprint. Discussion started: 31 March 2026
© Author(s) 2026. CC BY 4.0 License.

5 Data records

For each simulation set, the hourly snapshots of velocity components (*u*, *v*), water depth *h* and water surface elevation *zs* are stored as netCDF4 files. The derived maximum water depth *hmax*, velocity magnitude *Umax* and water surface elevation maps *zsmax* reached at each grid cell over the full simulation period are stored in separate GeoTIFF format and combined in a single .zip archive for each simulation case. The files are provided at the finest simulation resolution (4 m or 8 m) and the coordinates are given in the New Zealand Transverse Mercator 2000 coordinate system (EPSG:2193). The elevations are expressed using the New Zealand Vertical Datum 2016 (NZVD2016).

6 Dataset quality and uncertainty assessment

6.1 Modelling limitations and internal variabilities

Internal variabilities refer here to the sensitivity of the simulations to modelling choices, uncertainties in the input and intrinsic model limitations. No systematic sensitivity analysis was led to assess characteristic model uncertainties and variability to input. Several sources of uncertainties and model limitations were nevertheless identified during preliminary tests prior to framework deployment, a posteriori validation of the simulations, or inferred from conceptual reasoning. The level of uncertainty and impact on the hydrodynamic simulations are classified as residual, low, moderate and major. The sources of uncertainties are detailed in this section and summarised in Table 2.

6.1.1 DEM resolution and conditioning

DEM conditioning. Hydraulics conditioning relies mostly on the OpenStreetMap land use and infrastructures (bridges, culverts…) to systematically identify structural river obstructions and effectively open waterways. However, recent infrastructure and water channel culverts can be unreferenced resulting in channel discontinuities and undesired runoff. An example of non-opened culvert is shown in Fig. 6. Where identified, physical obstructions (e.g. culverts) were opened as part of the DEM hydraulic conditioning and updated in the OpenStreetMap database, however some remain. Similarly, partially or fully underground channels can be unreferenced, introducing uncertainties in the maximum flood depth exceeding 0.5m. Current efforts focus on addressing this limitation. Strategies considered include the implementation of available drainage network data during the DEM's hydraulics conditioning and representing culverts and underground channels as 1D hydraulic connectors within the hydrodynamic model. Overall the level of uncertainty introduced by the DEM conditioning is low, with moderate impact on the hydrodynamic simulations.

https://doi.org/10.5194/essd-2026-56
Preprint. Discussion started: 31 March 2026
© Author(s) 2026. CC BY 4.0 License.

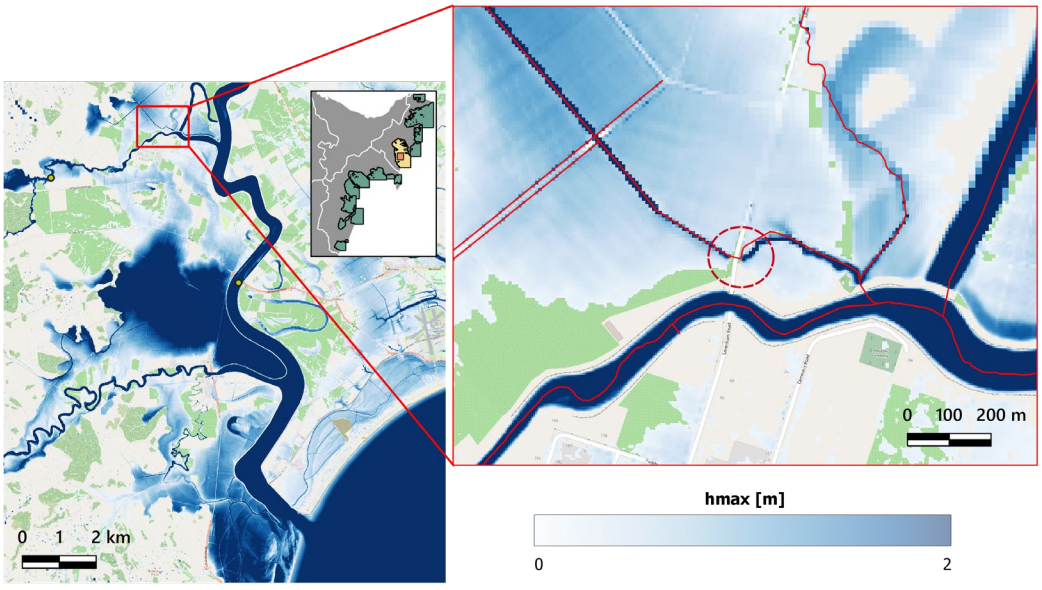

315 **Figure 5: Illustration of missing culvert in the Gisborne domain. The red lines identify the rural drains network (Gisborne District Council, 2023) and a non-opened culvert by the dashed circle. Background imagery ©OpenStreetMap.**

DEM resolution. As introduced in Sect. 3.4, 8 m resolution DEM can result in meaningful smoothing of levees. Simulations obtained using the initial 8 m resolution DEM and the corrected DEM in the Heretaunga Plains (4 m DEM) and Gisborne domains (8 m with corrected levees' crest elevation) were compared. While moderate differences were appreciable in terms 320 of flood extent, the corrections generally reduced maximum flood depth up to 0.5 m in the vicinity of some of the overtopped riverbanks. After levee conditioning, the DEM resolution uncertainty is considered low with residual impacts.

Surface roughness and friction model. The surface roughness is directly derived from the aggregation of subgrid scale characteristic elevation values and land use, with low to moderate uncertainty in the input datasets. Although the surface roughness has second order impacts on the simulation results compared to terrain constraints, they nevertheless show high 325 sensibility to the model chosen. As such, preliminary tests in the intricate flows of the Heretaunga Plains showed that the dynamic Smart model offer similar performances as the static Manning model in shallow waters. However, due to the model's ability to dynamically adjust Manning's coefficient with the water depth, the Smart model consistently outperforms the static model in rapid deep river flows where the latter generally overestimates surface friction and spilling. As a consequence, the uncertainty introduced by the surface roughness is considered moderate with low to moderate impacts when used in 330 conjunction with the dynamic Smart model.

6.1.2 Hydraulic forcing

Gridded rainfall interpolation. Gridded rainfall is generated from a limited number of rainfall gauges. In average, the domains are covered by 0.6 rainfall station per 100 km^2 and the most densely covered is the Aropaoanui catchment with less

https://doi.org/10.5194/essd-2026-56
Preprint. Discussion started: 31 March 2026
© Author(s) 2026. CC BY 4.0 License.

than 1.5 station per 100 km^2. The uncertainty introduced by the rainfall measurements is therefore considered to be high and directly propagates into the gridded rainfall interpolation. In addition, moderate uncertainty is also introduced by the NZCSM synoptic prediction used to guide the interpolation. Indeed, the synoptic prediction of the event aligns generally well with the recorded rainfall patterns. However, a posteriori analysis point at difficulties to accurately capture the cyclone pathway above mountain ranges and major impacts on the hydrodynamic simulation results. For instance, the NZCSM forecast predicted local rainfall peaks in the mountain ranges feeding into the Waiapu and Tolaga Bay catchments (North of the regions) which propagate into the interpolated gridded VCSN estimate. Rain gauge observations corroborate this high rainfall but slightly further South than the forecast, resulting in an overestimation of the rainfall forcing in the Waiapu catchment and the adjacent North section of the Tolaga Bay catchment while underestimating rainfall in the Western section of the Tolaga Bay catchment. Comparison of the baseline simulations against available river gauges records and aerial imagery localise major impacts due to rainfall inaccuracies in the vicinity of the Raukūmara and the northern section of the Kaimanawa mountain ranges longing the Eastern border of the Tairāwhiti regional district. Thus, meaningful under- or over-predictions of the hydraulic forcings are observed in the Waiapu, Tolaga Bay, Gisborne and Wairoa catchments (Fig. 1b), with peak water depth predictions exceeding ±1 m at the lowest reaches of the main rivers and flood extents overestimation exceeding 100 m in grassland of the Waiapu domain. Impacts are also expected to spread to the neighbouring domains of Tokomaru Bay and Waiomoko, where flood extents appear overpredicted in the vicinity of the main rivers' lower reaches, as well as the Mahia Beach and Nuhaka to a lesser degree. Aggregated together, uncertainties introduced by the VCSN gridded interpolated rainfall are major, with major impacts in the Tairāwhiti domains, moderate impacts in the Northern Hawke's Bay domains and residual to low impacts elsewhere. Calibration mainly aimed to correct the error introduced by the rainfall interpolation uncertainty.

Hydrological model. Uncertainties in the hydrological model are residual compared to the other uncertainties. While the rainfall forcing uncertainties propagate into the TopNet hydrological model, they are not expected to grow beyond the magnitude of the initial rainfall uncertainties.

6.1.3 Hydrodynamic model

Rheology, sediment transport and morphology changes. In locations, morphological changes of the terrain (e.g. erosion/aggradation, debris accumulation along obstacles, levee breaches), together with large amount of sediments carried by the river streams during the event (e.g. landslides, river bank failures, bed erosion) strongly influenced the rivers' hydrodynamics in ways not represented by BG-Flood, with major impact on the simulation results. This can result in inherent deficiencies of the hydrodynamic model. Capturing these processes requires the detailed mapping of the underlying geophysical drivers (e.g. geology, topography, slope stability) at a level of spatial and temporal resolution not available introducing major uncertinty. In addition, the hydrodynamics solver would require substantial enhancement to implement additional physics, whether explicitly through the coupling with additional governing equations, or implicitly via the use of analytical or empirical parameterization. Overall, the impacts appear low at the peak of the event in most domains except in the Esk Valley in the Aropaoanui domain, where sediment deposits exceeding 2m were reported (Hawke's Bay Regional

https://doi.org/10.5194/essd-2026-56
Preprint. Discussion started: 31 March 2026
© Author(s) 2026. CC BY 4.0 License.

Council, 2024) (see difference between pre- and post-event DEMs in Fig. 6) and in the Dartmoor fields in the Heretaunga Plains where sediment deposits exceeding 0.5m of turbid water to runoff. Overall, rheological and morphological uncertainties are major, with low to moderate impacts on the simulations at the peak of the event in most domains, and major impacts localised in the Esk Valley.

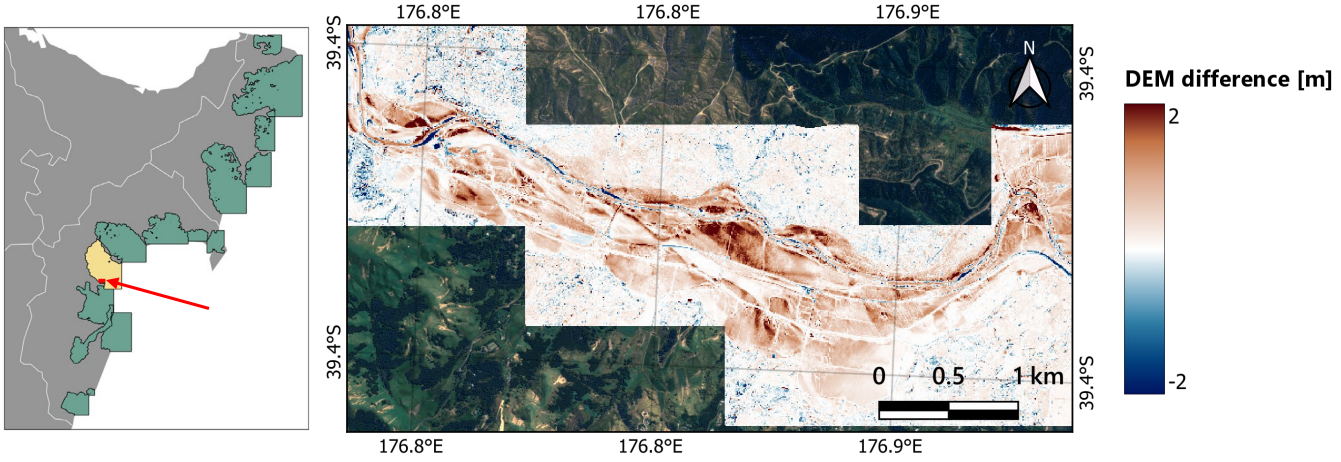

Figure 6: Elevation difference between 8 m resolution post- and pre-event DEMs in the Esk Valley (Aropaoanui domain). Red indicates aggradation and blue erosion. Background imagery © Land Information New Zealand (LINZ), CC BY 4.0 (Toitū Te Whenua – Land Information New Zealand Data Service (LINZ), 2023c).

Surface infiltration. Initial and continuous infiltrations are neglected in the hydrodynamic models. This is justified by the generally wet conditions preceding the event and the high rainfall rate rapidly saturating the soil at the start of the event, forcing rainfall to drain as surface runoff. Additionally, the implementation of stormwater and underground drainage networks to model urban flooding is a well-documented source of uncertainty, and, if ignored, can lead to major flood overpredictions. These are often represented as infiltration coefficients or directly in the governing equations as infiltration fluxes which parametrization can vary according to the urban land use and drains network (Ming et al., 2025). In our cases, existing stormwater networks were designed to sustain 0.1% to 0.05% annual exceedance probability events. Where existing (e.g. Gisborne, Napier) they were rapidly overwhelmed by the extreme rainfall and played a low if not residual role in mitigating urban flooding. Together, uncertainties introduced by neglecting surface infiltration and stormwater drainage networks are considered moderate, with residual impacts during the peak of the event.

6.1.4 Grid refinement map

The grid refinement map is designed to balance accuracy and computational cost. Levees are resolved at 4 m resolution, providing high confidence in crest elevation and overtopping representation. Along the major rivers without levees, 8 m resolution is found sufficient to capture channel shape and floodplain runoff sources. In the upper reaches of the domains, where the terrain is steep and less impactful on the downstream flood hydrodynamics, channels can be represented at 16 m resolution. In these areas, bank smoothing can occasionally favour early spilling. However, the effects are generally small

https://doi.org/10.5194/essd-2026-56
Preprint. Discussion started: 31 March 2026
© Author(s) 2026. CC BY 4.0 License.

(typically lower than 0.5 m water depth) and have negligible influence on the downstream floodplain hydrodynamics and flood hazards. In floodplains where flow velocities are low, narrow channels (small water streams and above ground drains) and surface runoff, are represented at 16 m resolution. Impacts are generally low, but occasionally cause moderate spilling caused by narrow channel smoothing (width < 8 m). Overall, the uncertainty associated with the refinement map are considered moderate with moderate impacts on the regions of interest.

Table 2. Uncertainty sources, impacts and confidence levels summary.

Uncertainty source	Description	Level of uncertainty	Impact on hydrodynamic simulations
DEM conditioning	Missing or unreferenced culverts, underground channels, and infrastructure in OSM can cause channel discontinuities and undesired runoff. Manual corrections applied where identified.	**Low to Moderate**	**Moderate** along unopened waterways (e.g. unreferenced culvert; >0.5 m water depth)
DEM resolution	8 m DEM smooths narrow levees; corrected using 4 m DEM (Heretaunga Plains) and levee crest adjustments (Gisborne).	**Low**	**Residual** after levee conditioning
Rainfall interpolation (VCSN)	Sparse gauge network (<1.5 stations/100 km²). Misplacement of rainfall maxima over mountain ranges leads to over/underestimation in several catchments.	**Major**	**Major** in Tairāwhiti (±1m depth, up to 100m flood extent errors). **Moderate** in Northern Hawke's Bay **Low** elsewhere.
Hydrological model (TopNet)	Rainfall uncertainties propagate into inflow hydrographs but do not amplify beyond rainfall uncertainty.	**Low**	**Residual to low** relative to other uncertainty sources.
Rheology, sediment transport, morphology	Erosion, aggradation, debris, levee breaches, and sediment-laden flows not represented by BG-Flood. Large morphological changes in Esk Valley.	**Major**	**Major** impacts in the Esk Valley (>2 m deposits; >1 m water depth error)
Surface infiltration	Infiltration neglected due to saturated soils and extreme rainfall. Stormwater networks rapidly overwhelmed; missing underground drains can cause local ponding.	**Moderate**	**Residual** impacts at the peak of the event
Grid refinement	4 m around levees; 8 m along major rivers; 16 m in steep upper reaches. Coarser grids may smooth banks, small rivers and favour early spilling.	**Moderate**	**Residual** along the main rivers **Moderate** in upper reaches and along narrow streams (<0.5m),

6.2 Technical validation

The regional inundation map obtained from aggregating the separate domains is shown in Fig. 7 and the validation process is illustrated for the Gisborne domain in Fig. 8. After calibration, the models produce satisfactory results. The predicted flood extents are accurately captured when compared to the aerial/satellite imagery, with overall qualitative agreement found between the predicted inland runoffs and the residual sediment trails left by river overflows. The predicted hydrographs also reproduce the rising limb and peak flow satisfactorily at the gauges as illustrated for the Gisborne domain in Fig. 8d. Calibration satisfyingly correct hydrographs at gauges as well as river overtopping and runoffs inaccurately captured by the baseline model as illustrated by the hydrographs of gauges (19766; 19737) (Fig. 8d) and the mismatch between the large sediment trails and flooded regions along Te Arai river, Gisborne, in Fig. 8b.

https://doi.org/10.5194/essd-2026-56
Preprint. Discussion started: 31 March 2026
© Author(s) 2026. CC BY 4.0 License.

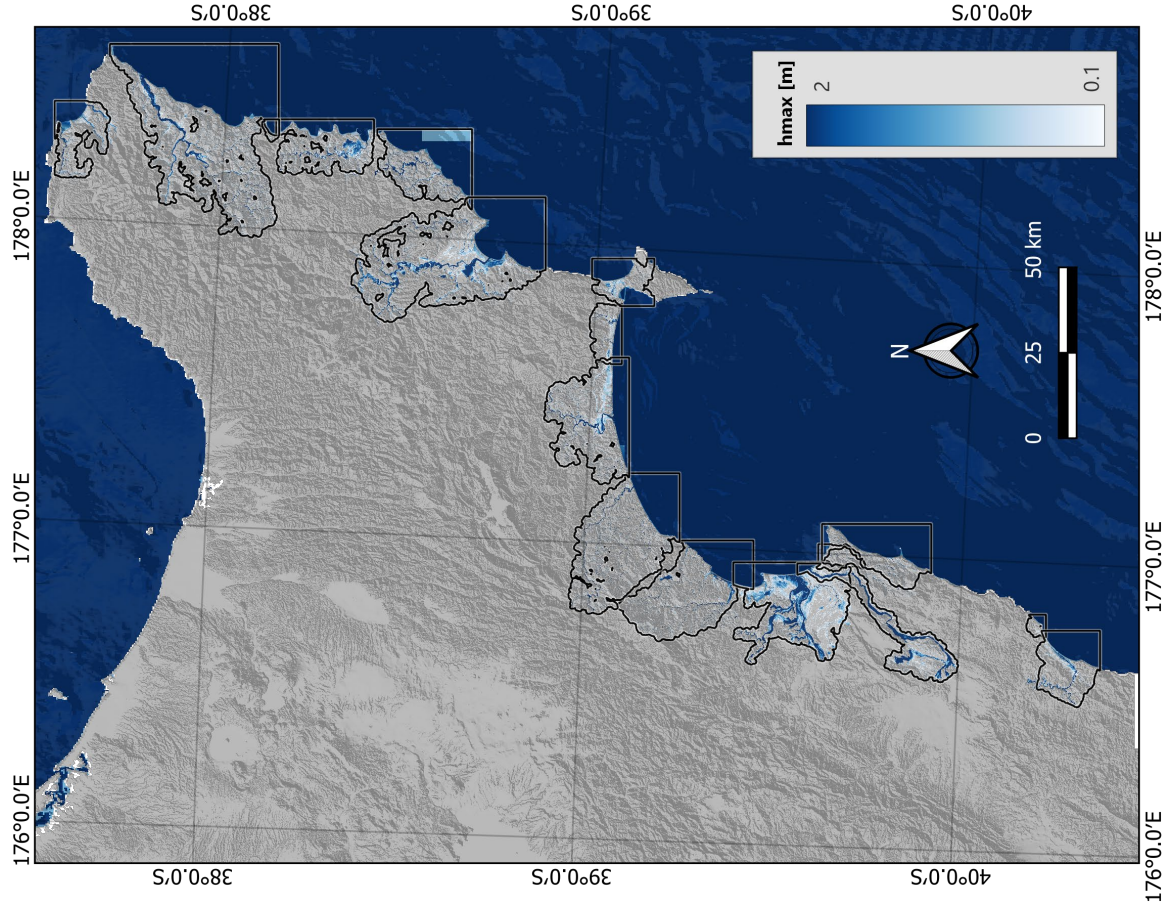

Figure 7: Regional flood map aggregating the maximum water depth achieved during the simulation period for the 16 domains.

The spatial distribution of prediction errors for the baseline and calibrated models in the Gisborne, Aropaoanui and Heretaunga Plains domains are shown in Fig. 9, and the corresponding KDE are show in Fig. 10. Overall, the baseline models compare well with the surveyed high-water marks in the Gisborne (Fig. 9a.1) and Heretaunga Plains (Fig. 9c.1) domains. This agreement is reflected in overall low biases – error distributions centred near zero –, with median values below 0.2 m and 80% central intervals mostly within the ±1 m error range (Fig. 9a and c). However, local discrepancies are identified in both cases. In Gisborne, the underestimation of the river spills and peak hydrograph at station 19766 identified in Fig. 8 correspond to systematic underpredictions ($\varepsilon < 0$) along the Te Arai River (Fig. 9a.1, South-West), primarily caused by rainfall misestimation. These are corrected by increasing the Te Arai River's injection flow by 75%. Similarly, in the Heretaunga Plains, local underpredictions appear immediately downstream of levee breaches (Fig. 9c, black circles – Dartmoor, North of the Tūtaekurī River, and Fernhill, along the Ngaruroro River), which are included in the calibrated model. Estimates of the locations and timings of the breaches were provided by the Hawke's Bay Regional Council, and locations were further refined using post-event imagery. In both cases, calibration (injections tuning in Gisborne, dynamic adaptation of the topography

https://doi.org/10.5194/essd-2026-56
Preprint. Discussion started: 31 March 2026
© Author(s) 2026. CC BY 4.0 License.

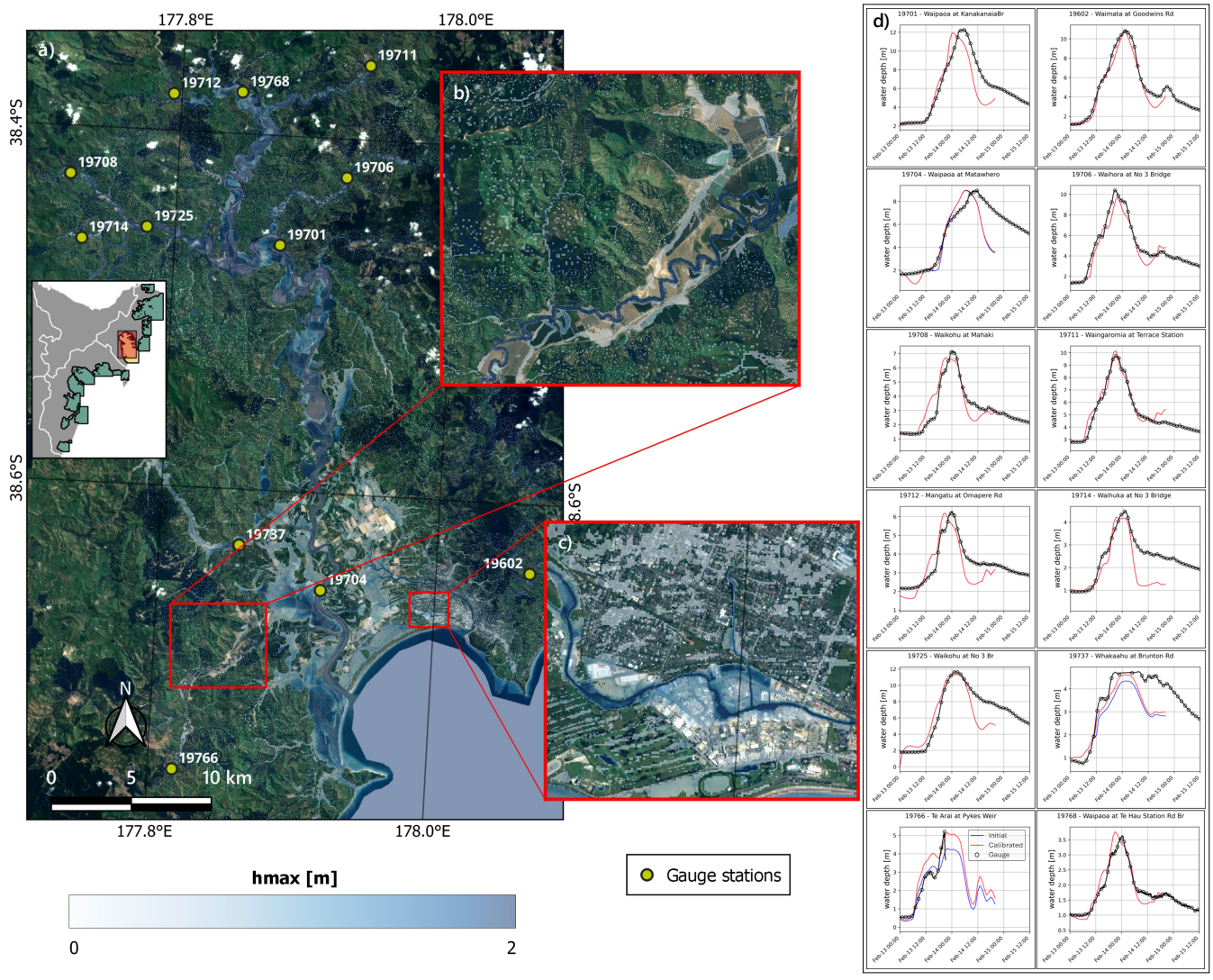

Figure 8: Predicted inundation map (*a*) and hydrographs at the gauges (*d*) for the Gisborne domain. The insets highlight underestimated overtopping along the Te Arai River and north (*b*) and floods in the Awapuni suburb of Gisborne city (*c*). The maximum water depth *hmax* is plotted with 50% transparency. Background imagery © Land Information New Zealand (LINZ), CC BY 4.0 (Toitū Te Whenua – Land Information New Zealand Data Service (LINZ), 2023c).

https://doi.org/10.5194/essd-2026-56
Preprint. Discussion started: 31 March 2026
© Author(s) 2026. CC BY 4.0 License.

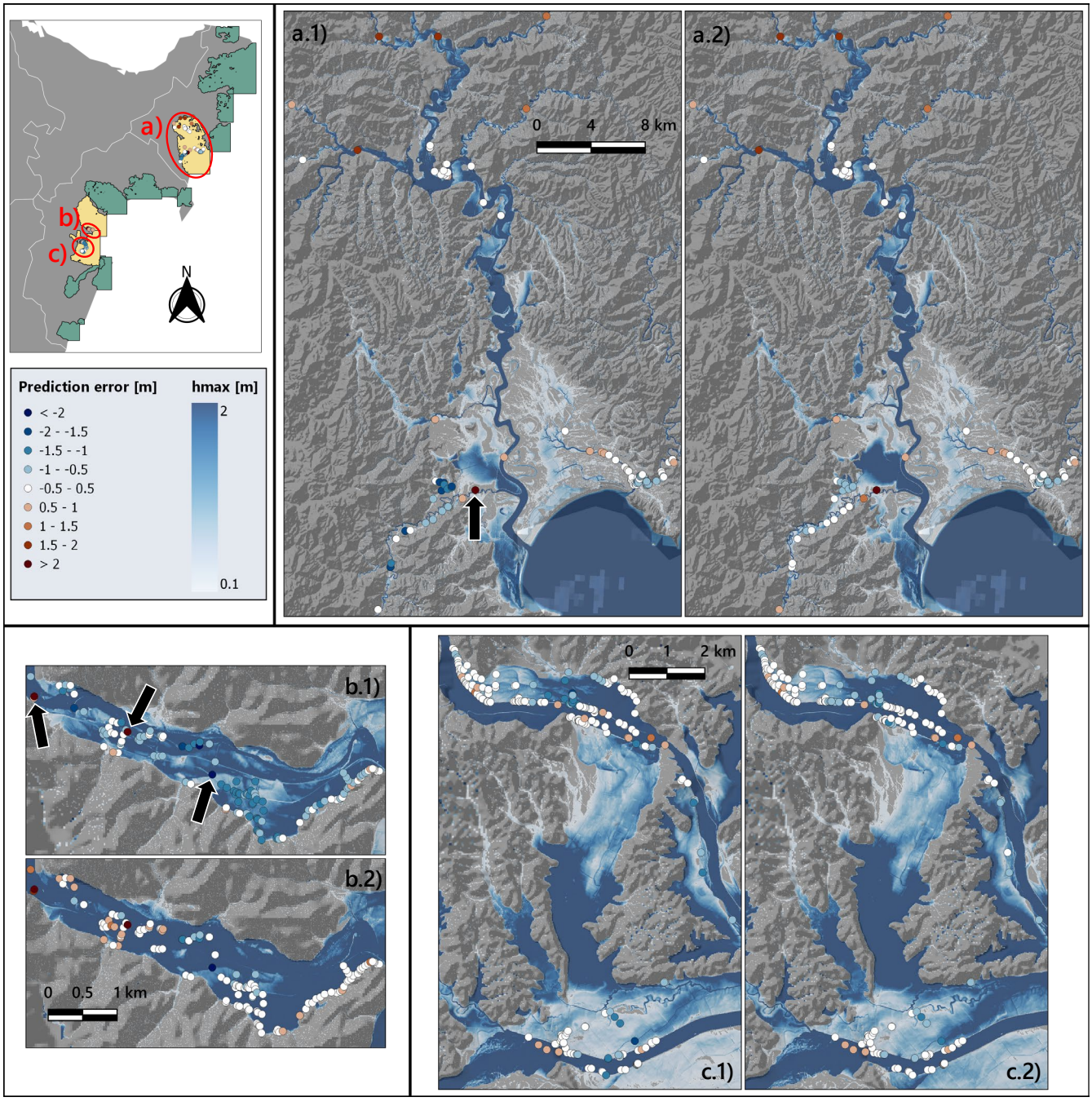

Figure 9: Prediction errors at the surveyed high-water marks in the Gisborne (*a.1,2*), Aropaoanui (*b.1,2*) and Heretaunga Plains (*c.1,2*) domains. The baseline models are identified by suffix (*.1*) and calibrated models by suffix (*.2*). The black arrows identify outliers.

https://doi.org/10.5194/essd-2026-56
Preprint. Discussion started: 31 March 2026
© Author(s) 2026. CC BY 4.0 License.

Open Access Earth System Science Data Discussions

The Esk Valley, located in the Aropaoanui domain (Fig. 9-10b), was among the most severely impacted during the event and the most challenging to calibrate. The baseline model systematically underpredicts water surface elevations, with $|\varepsilon| > 0.5\ m$ at over half of the surveyed points. This bias is attributed to: (i) the substantial transport and deposition of alluvium and debris over the valley floor as introduced in Sect. 6.1.3; (ii) a misplacement of rainfall peaks across the catchment led to excess discharge of the Esk River and insufficient rainfall over the Aropaoanui River catchment (Sect. 0), partly mitigating underpredictions due to inaccurate physics representation.

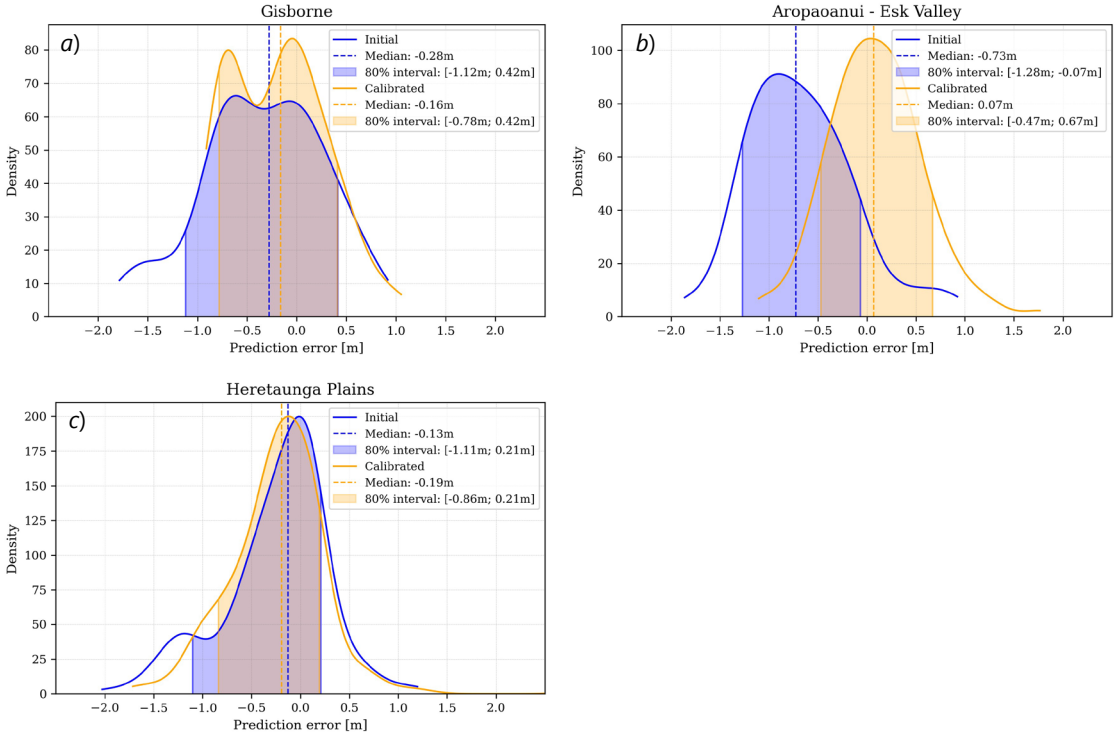

Figure 10: Prediction errors intensity estimates at surveyed high-water marks for the separate Gisborne (*a*), Aropaoanui (*b*) and Heretaunga Plains (*c*) domains for the baseline and calibrated models.

Calibration efforts focus on a subdomain covering the lower Esk Valley, and attempt to adjust the boundary hydrograph at the valley inlet to compensate for the inherent deficiencies of the numerical solver. The calibrated model produces substantial improvement at the surveyed high-water marks. The increased river discharge results in a systematic increase of the water level, with a meaningful suppression of bias characterised by the shift of the median from -0.73 m to 0.07 m, and the tightening of the 80% central interval – more than 70% of the points falling in the ±0.5 m error range (Fig. 10b). It is important to note that the quality of the calibrated model is to be understood rather qualitatively than as an accurate picture of the actual dynamics during the event. Indeed, limitations of the calibration approach is striking upon close comparison of the errors' spatial distribution across the valley between baseline and calibrated models (Fig. 9b). Calibration gains at the lower section of the valley were obtained at the cost of slightly overpredicting in the upper valley where the baseline model performed well. As

https://doi.org/10.5194/essd-2026-56
Preprint. Discussion started: 31 March 2026
© Author(s) 2026. CC BY 4.0 License.

Open Access Earth System Science Data Discussions

introduced in Sect. 6.1.3, adequate representation of the Esk Valley's dynamics far exceeds the scope of this project given the hydrodynamics solvers capabilities (no sediment dynamics) and the time required to calibrate the underlying geophysical drivers responsible for alluvium and coarse debris load.

https://doi.org/10.5194/essd-2026-56
Preprint. Discussion started: 31 March 2026
© Author(s) 2026. CC BY 4.0 License.

Table 3. Domain-by-domain simulation summary for Tairāwhiti. The DEM conditioning and sediment load sources of uncertainties are not indicated as they apply to all domains. Best scenarios capturing the conditions during the event are in bold font in the Scenario cases column. Confidence in the simulation output is classified as low, moderate and high. HWM refers to High Water Marks.

Domains	Dominant uncertainties	Simulation cases	Comments	Confidence
Te Araroa	Rainfall interpolation No gauge or HWM	**Baseline model**	Flood extent overestimated in all rivers' lowest reaches	**Low**
Waiapu	Rainfall interpolation	Baseline model	Large overpredictions of the flood extent and peak water depth >1.5 m at the lowest gauge.	**Low**
		Intermediate cases. Scaling of all injections (75%, 45%)	Good peak water depth at the gauge but inconsistent improvements of the flood extent along the Waiapu River	**Low**
		Calibrated model. Modelling of the entire catchment (no injections) with scaled hourly gridded rainfall (50%)	Best prediction at the gauge and good match with sediment trails with local inconsistencies	**Moderate**
Tokomaru Bay	Rainfall interpolation No gauge or HWM	**Baseline model**	Flood extent overestimated in all rivers' lowest reaches	**Moderate**
Tolaga Bay	Rainfall interpolation + Injection hydrographs No gauge or HWM	Baseline model	Flood extent underpredicted along the Mangaheia River flowing from the Western side of the domains, and generally overpredicted elsewhere	**Low**
		Calibrated model. Scaling of Mangaheia River injections (150%) Scaling of remaining injections (70%)	Overall good estimation of the flood extent except local discrepancies	**Moderate**
Waiomoko	Rainfall interpolation No gauge or HWM	**Baseline model**	Moderate overprediction of water spill in the valley leading to the Bay.	**Moderate**
Gisborne	Rainfall interpolation Urban drainage networks	Baseline model. 8 m DEM with conditioned levees' crest elevation	Satisfying match at gauges and HWM. Underpredictions along the Te Arai River flowing from the South-East	**Moderate**
		Calibrated model. Scaling of the Te Arai River injections (175%)	Satisfying correction of the Te Arai River flow	**High**

Open Access Earth System Science Data Discussions

https://doi.org/10.5194/essd-2026-56
Preprint. Discussion started: 31 March 2026
© Author(s) 2026. CC BY 4.0 License.

Table 3. (Continued) Domain-by-domain simulation summary for Hawke's Bay.

Domains	Dominant uncertainties	Simulation cases	Comments	Confidence
Mahia Beach	No gauge or HWM	**Baseline model**	Apparent good estimate of flood extents. Note, the sediment trails are difficult to identify on the 0.5m satellite imagery over certain vegetations in the 0.5 m satellite imagery (Toitū Te Whenua – Land Information New Zealand Data Service (LINZ), 2023c)	**Moderate**
Nuhaka	No gauge or HWM	**Baseline model**	Overall good match with sediment trails. Runoff in populated area seem to match with reported runoff in the Nuhaka School	**Moderate**
Wairoa	Rainfall interpolation Injection hydrographs	Baseline model	Complex river configuration with 2 connected sharp elbows causing frequent flooding. Large spilling overprediction in the North Clyde and Wairoa populated centres	**Low**
		Calibrated model. Scaling of all injections (65%)	Improved representation of the flood event	**High**
Mohaka	No gauge or HWM	**Baseline model**	Good alignment of the water pathway with sediment deposits	**Moderate**
Aropaoanui	Rainfall interpolation Rheology/morphology	Baseline model	Aropaonui River. Good alignment of the water pathway with sediment deposits. Maximum water depth match with collected photos and population reports at the Tangoio community Marae longing the river Esk Valley. Large sediment loads lead to consistent max. water depths underpredictions at the HWM (>0.5 m).	**Low**
		Calibrated model. Domain focused on the Esk Valley with injections calibrated to match gauge records at the Valley entrance	Overall improvement of the max. depth at the HWM, but low confidence in the dynamics during the event	**Moderate to Low**
Heretaunga Plains	Levee breaching Urban drainage networks	Baseline model. 4 m DEM + 4 m surface roughness at Redclyffe bridge Bridge to represent partial obstruction of the Tūtaekurī River	Overall good capture of the flood extent and hydrographs at the gauges. The absence of the levee breaches induces underestimates of water spilling along the upper reaches of the Ngaruroro and Tūtaekurī Rivers and urban flooding overestimates in the lower reaches	**Moderate**
		Calibrated model. Dynamic adjustment of the topography to implement levee breaches during the simulation period	Overall improvement of the peak water depth at the gauges and HWM (error < 0.8 m). Reduction of urban flooding in Taradale in agreement with photos shared by the Hawke's Bay regional council	**High**
		Glass wall scenarios**.** Levees are made impermeable	Scenario designed to investigate the total load of the Tūtaekurī and Ngaruroro Rivers	**N/A**
Tukituki		**Baseline model**	The wider bed of the Tukituki River is constrained in its valley, then by levees after exiting the valley Good match of the hydrograph at Red Bridge with peak depth difference < 0.2 m Large runoff towards Otane captured	**High**
		Scenario. Artificial wall added to the DEM to block Waipawa River runoff towards Pourerere road	Scenario designed to investigate the response total load of the Tukituki river without the Otane runoff	**N/A**
Maraetotara-Waimarama	No gauge or HWM	**Baseline model**	Apparent good matchwith sediment trails in Te Awanga (Lower Maraetotara River) No probant conclusion for the Waimarama River	**Moderate**
Waikaraka	No gauge or HWM	**Baseline model**	Difficult to identify sediment trails from vegetation on 0.5 m satellite imagery. Moderate confidence attributed on the basis of the high confidence in the Pōrangahau domain	**Moderate**
Pōrangahau		**Baseline model**	Good match between sediment trails and flood extent across croplands	**High**

Open Access Earth System Science Data Discussions

https://doi.org/10.5194/essd-2026-56
Preprint. Discussion started: 31 March 2026
© Author(s) 2026. CC BY 4.0 License.


7 Data availability

The flood hazard simulation dataset presented in this study is publicly accessible at https://doi.org/10.5281/zenodo.17986628 (Pelmard, 2025a) for the Tairāwhiti regional district and https://doi.org/10.5281/zenodo.18001575 (Pelmard, 2025b) for the Hawke's Bay regional district. The archive includes all model outputs presented in this paper, along with accompanying metadata and documentation. All data are available under the CC BY 4.0 copyright policy with appropriate citations of this paper.

8 Summary and conclusions

This study presents a comprehensive dataset of flood hazard simulations for 16 floodplains across the Hawke's Bay and Tairāwhiti regions during ex-Tropical Cyclone Gabrielle. The modelling framework integrates the rainfall records interpolation into gridded datasets, hydraulic conditioning of elevation datasets, hydrological runoff modelling, and multi-resolution GPU-accelerated hydrodynamic modelling to produce spatially and temporally resolved inundation maps. Validation against hydrograph records, aerial imagery, and high-water mark surveys demonstrates the framework's capacity to capture key flood dynamics across diverse catchments.

While minimal calibration successfully corrects local discrepancies growing from area specific features (e.g. levee breaches) and inaccuracies in the rainfall interpolation, inherent limitations of the modelling methods restrict improvement in locations where high alluvium and coarse debris loads (e.g. Esk Valley) or urban drainage networks significantly influenced the flow dynamics.

Building on the framework's modular design, several directions of expansion are underway. Following validation against Cyclone Gabrielle, the framework is being deployed to develop a nationwide dataset of flood models covering over 250 floodplains. Initial applications focused on 1% annual exceedance probability (AEP) design storms under present-day climate, projected temperature increase and sea-level rise conditions (see project https://niwa.co.nz/hazards/ma-te-haumaru-o-nga-puna-wai-o-rakaihautu-ka-ora-mo-ake-tonu), and ongoing simulations extend the database to 10–0.1% AEP events, enabling a matrix of future flood risk scenarios. These datasets are in turn used to generate risk-oriented analysis of flood impacts (e.g. damage/cost analysis), and the production of annualised aggregated output at regional- and national-scale to support comprehensive assessments of flood impacts across Aotearoa New Zealand. Additional works also aim to adapt the framework for operational real-time flood forecasting to enhance early warning capabilities.

The dataset offers a valuable resource for post-event analysis, damage and infrastructure resilience assessment, and future scenario modelling. By bridging detailed hydrodynamic modelling with regional-scale hazard assessment, this work contributes to the growing need for robust, data-driven tools in climate resilience and disaster response planning.

https://doi.org/10.5194/essd-2026-56
Preprint. Discussion started: 31 March 2026
© Author(s) 2026. CC BY 4.0 License.

9 Authors contributions

JP designed the numerical models, led the simulations, validation, model calibration and data analysis, curated the dataset and led the manuscript writing. EL conceptualised the project, was main project supervisor and administrator, performed tide modelling and hydrological modelling, and contributed to the manuscript preparation. AH assisted in the design of the numerical models, performed simulations, model calibration, data analysis, and contributed to the manuscript preparation. CB created the hydrodynamic solver, assisted in the design of the numerical models, conceptualised the project and contributed to the manuscript preparation. ZX contributed to the design of the numerical models, performed simulations, validation, calibration and data analysis. RP (Pearson) created the Geofabrics procedure and generated the hydraulically conditioned ground elevation dataset. TCS created the VCSN gridded rainfall for the event and contributed to the manuscript preparation. GS surveyed and curated the high-water marks dataset, assisted in data analysis and contributed to the manuscript preparation. JB surveyed and curated the high-water marks dataset. RP (Paulik) performed data analysis and contributed to the manuscript preparation. RK, EC and GB performed simulations, validation, model calibration and data analysis. CZ was project supervisor and contributed to the manuscript preparation. LW was project administrator and contributed to the manuscript preparation.

10 Competing interests

The authors declare having no competing interests.

11 Financial support

Funding for the Rapid Flood Hazard Assessment and Modelling for Cyclone Gabrielle Recovery project was provided by the Ministry for Business Innovation and Employment (MBIE) Strategic Science Investment Fund (SSIF) through the Extreme Weather Research Platform.

12 Acknowledgement

The analysis was partly undertaken using a High-Performance Computing (HPC) platform provided by the New Zealand eScience Infrastructure (NeSI) consortium. We thank Craig Goodier (Principal Engineer at the Hawke's Bay Regional Council) and Murry Cave (Principal Scientist at the Gisborne District Council) and their respective teams for their collaboration, data sharing and expert advice in interpreting the results. We also acknowledge the contributions of our WSP partners Liam Foster, Isabelle Farley and Harm van Oorschot to the simulation process.

https://doi.org/10.5194/essd-2026-56
Preprint. Discussion started: 31 March 2026
© Author(s) 2026. CC BY 4.0 License.

References

Bosserelle, C., Williams, S., Cheung, K. F., Lay, T., Yamazaki, Y., Simi, T., Roeber, V., Lane, E., Paulik, R., and Simanu, L.: Effects of Source Faulting and Fringing Reefs on the 2009 South Pacific Tsunami Inundation in Southeast Upolu, Samoa, J. Geophys. Res. Oceans, 125, e2020JC016537, doi:10.1029/2020JC016537, 2020.

Crawford-Flett, K., Blake, D. M., Pascoal, E., Wilson, M., and Wotherspoon, L.: A standardised inventory for New Zealand's stopbank (levee) network and its application for natural hazard exposure assessments, J. Flood Risk Manag., 15, e12777, doi:10.1111/jfr3.12777, 2022.

Earth Sciences New Zealand: River Environment Classification 2.5 [dataset], https://dc.niwa.co.nz:/niwa_dc/srv/api/records/0abeee37-9805-459a-8c9f-b0f488775aa0/, 2022.

Gisborne District Council: Gisborne District Rural Drains, Gisborne District Council [dataset], https://geoportal-gizzy.opendata.arcgis.com/datasets/gizzy::rural-drains/, 2023.

Gisborne District Council and Toitū Te Whenua – Land Information New Zealand (LINZ): LiDAR dataset, Gisborne, New Zealand 2018-2020 [dataset], doi:10.5069/G92V2D9X, 2021.

Hawke's Bay Regional Council: Report of the Hawke's Bay Independent Flood Review - Pae Matawai Parawhenua, https://www.hbrc.govt.nz/our-council/hb-independent-flood-review/, 2024.

Hawke's Bay Regional Council, Wairoa District Council, Hastings District Council, Napier City Council, Central Hawke's Bay District Council, and Toitū Te Whenua – Land Information New Zealand Data Service (LINZ): LiDAR dataset, Hawke's Bay, New Zealand 2020-2021 [dataset], doi:10.5069/G9S75DH2, 2023.

Lane, E. M. and Walters, R. A.: Verification of RiCOM for Storm Surge Forecasting, Mar. Geod., 32, 118-132, doi:10.1080/01490410902869227, 2009.

Lane, E. M., Walters, R. A., Gillibrand, P. A., and Uddstrom, M.: Operational forecasting of sea level height using an unstructured grid ocean model, Ocean Model., 28, 88-96, doi:10.1016/j.ocemod.2008.11.004, 2009.

Leith, K., McColl, S., Robinson, T., Massey, C., Smith, H., Wotherspoon, L., Carey-Smith, T., Ashraf, S., Barrell, D., Betts, H., Bidmead, J., Boyes, A. F., Bruce, Z., Buxton, R., Daysh, I., Dreyer, L., Easterbrook-Clarke, L., Farr, J., Glassey, P., Gnesko, L., Harvey, J., Heron, D., Hill, M., Jaramillo, A., Jones, K., Knoltsch, A., Lawson, R. V., Lee, J., Lin, A., Lukovic, B., L., H., Pelmard, J., Pola, A., Rosser, B., Rozmus, K., Tamang, N. B., Townsend, D., de Vilder, S., Wight, J., Wolter, A., Zhou, H., and Zoeller, A.: 2023 Cyclone Gabrielle Landslide Data [dataset], doi:10.17605/OSF.IO/QBMD9, 2025.

Massey, C., Leith, K., Robinson, T. R., Lukovic, B., McColl, S., Carey-Smith, T., Rosser, B., Wotherspoon, L., Smith, H., Betts, H., Buxton, R., and Bidmead, J.: What controlled the occurrence of more than 116,000 human-mapped landslides triggered by Cyclone Gabrielle, New Zealand?, Landslides, doi:10.1007/s10346-025-02591-y, 2025.

McMillan, H. K., Booker, D. J., and Cattoën, C.: Validation of a national hydrological model, J. Hydrol., 541, 800-815, doi:10.1016/j.jhydrol.2016.07.043, 2016.

Ming, X., Liang, Q., and Jiang, J.: Large-scale high-resolution hydrodynamic modelling of urban floods: Some practical considerations, Journal of Hydro-environment Research, 59, 100655, doi:https://doi.org/10.1016/j.jher.2025.100655, 2025.

Neal, J., Hawker, L., Savage, J., Durand, M., Bates, P., and Sampson, C.: Estimating River Channel Bathymetry in Large Scale Flood Inundation Models, Water Resour. Res., 57, e2020WR028301, doi:10.1029/2020WR028301, 2021.

Oliver, H., Shin, M., Matthews, D., Sanders, O., Bartholomew, S., Clark, A., Fitzpatrick, B., van Haren, R., Hut, R., and Drost, N.: Workflow Automation for Cycling Systems, CiSE, 21, 7-21, doi:10.1109/MCSE.2019.2906593, 2019.

Oliver, H. J., Shin, M., and Sanders, O.: Cylc: A Workflow Engine for Cycling Systems, J. Open Source Softw., 3, 737, doi:10.21105/joss.00737, 2018.

https://doi.org/10.5194/essd-2026-56
Preprint. Discussion started: 31 March 2026
© Author(s) 2026. CC BY 4.0 License.

Pearson, R. A., Smart, G., Wilkins, M., Lane, E., Harang, A., Bosserelle, C., Cattoën, C., and Measures, R.: GeoFabrics 1.0.0: An open-source Python package for automatic hydrological conditioning of digital elevation models for flood modelling, Environ. Model. Softw., 170, 105842, doi:10.1016/j.envsoft.2023.105842, 2023.

Pelmard, J., Harang, A., Bosserelle, C., Pearson, R., Carey-Smith, T., Lane, E. M.: Multi-Scenario Flood Simulations Dataset for 2023 ex-Tropical Cyclone Gabrielle in Tairāwhiti, Aotearoa New Zealand [dataset], doi:10.5281/zenodo.17986628, 2025a.

Pelmard, J., Harang, A., Bosserelle, C., Pearson, R., Carey-Smith, T., Lane, E. M.: Multi-Scenario Flood Simulations Dataset for 2023 ex-Tropical Cyclone Gabrielle in Hawke's Bay, Aotearoa New Zealand [dataset], doi:10.5281/zenodo.18001575, 2025b.

Popinet, S.: Quadtree-adaptive tsunami modelling, Ocean Dyn., 61, 1261-1285, doi:10.1007/s10236-011-0438-z, 2011.

Revell, M., Carey-Smith, T., and Moore, S.: A severe frontal rain event over the lower North Island of New Zealand with intense embedded convective banding, Weather and Climate, 39, 14-27, doi:10.2307/26892909, 2019.

Smart, G. M.: An improved flow resistance formula, Riverflow2004, Naples, 259-263, 2004.

Smart, G. M.: Improving flood hazard prediction models, Int. J. River Basin Manag., 16, 449-456, doi:10.1080/15715124.2017.1411923, 2018.

Stats NZ – Tatauranga Aotearoa (n.d.): Population, https://www.stats.govt.nz/topics/population/, 2023.

Tait, A., Henderson, R., Turner, R., and Zheng, X.: Thin plate smoothing spline interpolation of daily rainfall for New Zealand using a climatological rainfall surface, Int. J. Climatol., 26, 2097-2115, doi:10.1002/joc.1350, 2006.

Te Kāhui Inihua o Aotearoa Insurance – Council of New Zealand 2023 climate disaster payouts top $2 billion, https://www.icnz.org.nz/industry/cost-of-natural-disasters/, 2023.

Te Kāhui Inihua o Aotearoa Insurance – Council of New Zealand Cost of natural disasters Table, https://www.icnz.org.nz/industry/cost-of-natural-disasters/, 2024.

Toitū Te Whenua – Land Information New Zealand Data Service (LINZ): Hawke's Bay 0.10m Cyclone Gabrielle Aerial Photos (2023) [dataset], https://data.linz.govt.nz/layer/112726-hawkes-bay-010m-cyclone-gabrielle-aerial-photos-2023/, 2023a.

Toitū Te Whenua – Land Information New Zealand Data Service (LINZ): Gisborne 0.2m Cyclone Gabrielle Aerial Photos (2023) [dataset], https://data.linz.govt.nz/layer/112864-gisborne-02m-cyclone-gabrielle-aerial-photos-2023/, 2023b.

Toitū Te Whenua – Land Information New Zealand Data Service (LINZ): North Island 0.5m Cyclone Gabrielle Satellite Imagery (2023) [dataset], https://data.linz.govt.nz/layer/112807-north-island-05m-cyclone-gabrielle-satellite-imagery-2023/, 2023c.

Trust Tairāwhiti: Economic baseline and Cyclone Gabrielle loss estimates, Trust Tairāwhiti, Regional Wellbeing – He Tohu Ora, https://trusttairawhiti.nz/assets/Resources/TT-Economic-baseline-and-loss-estimates-280723PWP2-FINAL-v2.pdf, 2023.

Vacondio, R., Dal Palù, A., Ferrari, A., Mignosa, P., Aureli, F., and Dazzi, S.: A non-uniform efficient grid type for GPU-parallel Shallow Water Equations models, Environ. Model. Softw., 88, 119-137, doi:10.1016/j.envsoft.2016.11.012, 2017.

Wilson, N., Broadbent, A., and Kerr, J.: Cyclone Gabrielle by the numbers - A review at six months, Public Health Communication Centre Aotearoa, https://www.phcc.org.nz/briefing/cyclone-gabrielle-numbers-review-six-months/, 2023.

Xu, Z., Bosserelle, C., and Lane, E.: Nearfield effects of the 2022 Hunga-Tonga volcanic tsunami and implications for a volcanic eruption near the coast, Ocean Eng., 321, 120465, doi:10.1016/j.oceaneng.2025.120465, 2025.